Changes to Grain Properties due to Breakage in a Sand Assembly using Synchrotron Tomography

Tabassom Afshar[1,*], *Mahdi Disfani*[2], *Guillermo Narsilio*[2], and *Arul Arulrajah*[1]

[1] Department of Civil & Construction Engineering, Faculty of Science, Engineering & Technology, Swinburne University of Technology, Hawthorn, Victoria, Australia
[2] Department of Infrastructure Engineering, Melbourne School of Engineering, The University of Melbourne, Parkville, Victoria, Australia

Abstract. Grain breakage is of paramount importance for understanding the behaviour of granular materials used in various engineering applications, such as pavements, roads, rail tracks, the oil and gas industry, and mineral processing. Changes to grain properties of a uniformly graded sand specimen stemming from breakage during compression were studied with the aid of three-dimensional Synchrotron Radiation-based Micro-Computed Tomography. The fast scanning and high-resolution 4D imaging were utilised to capture images from the interior body of the granular assembly during loading. The fractal distribution of the sand assembly showed that breakage becomes dominant in smaller grains rather than larger ones, where an increase in the amount of newly generated fine fragments leads to high coordination number surrounding the larger grains. More importantly, the results of morphological changes in the particulate assembly revealed that there is a reversal trend in the grain morphology evolution with increasing stress. The sand grains tended to create more spherical fragments with higher aspect ratio whereas by increasing the stress this trend completely shifted.

1 Introduction

Grain breakage is common in granular materials, such as powders, soils, and manufactured aggregates, when subjected to high loading or large deformations. While breakage is desirable in some industries such as comminution in mineral processing [1], it may cause accelerated degradation of civil infrastructure, such as roads and pavement layers or ballast rail tracks [2], or decreases in the recovery rate in the oil and gas industry due to proppant crushing [3]. Grain breakage brings about changes in characteristics of granular materials, especially in grain size distribution and grain morphology. These shifts affect the mechanical behaviour of granular media and most prominently the material's crushing strength against further breakage [4].

While there are several studies on single-particle fracture mechanism and crack propagation (e.g. [5] and [6]), due to testing difficulties and the time-consuming steps of X-ray imaging, research on the impact of breakage on grain properties (particularly changes in grain morphology) in confined assemblies of individual grains is limited.

In this study, in order to obtain a better understanding of sand behaviours in relation to grain-scale damage, a novel loading apparatus capable of conducting compression tests at the high stress on assemblies of grains was designed and developed. Synchrotron Radiation-based X-ray Micro-Computed Tomography (SR-μCT) was used to capture high-resolution 4D images (i.e. 3D monitoring over time) from a sand assembly subjected to compression at different loads.

2 Experimental Method

A loading apparatus was developed in order to apply one-dimensional compression to the confined granular sand sample. The apparatus consists of two major parts: a sample chamber and a loading and data acquisition system (Figure 1). The sample chamber was made of a high-strength radiolucent tube of aluminium with a thickness of 5 mm, 25 mm internal diameter and 25 mm height. The load was applied manually using a reaction frame and screw. A Linear Variable Differential Transducer (LVDT) was used to measure deformation while a load cell continuously recorded the force.

The synchrotron facilities used in this study, in contrast with laboratory scanners, provide a monochromatic and highly culminated source of X-ray allowing high resolution imaging and also much more rapid scanning of samples loaded in high pressure metallic chambers. The vertical beam size of Hutch 3B of the Australian Synchrotron used in this study is approximately 25 mm, and the scans were conducted using a Ruby detector. Ruby is a custom designed detector of the Australian Synchrotron [7]. Resolutions of 11.6 μm were obtained in this study for the 25 mm samples tested.

* Corresponding author: tafshar@swin.edu.au

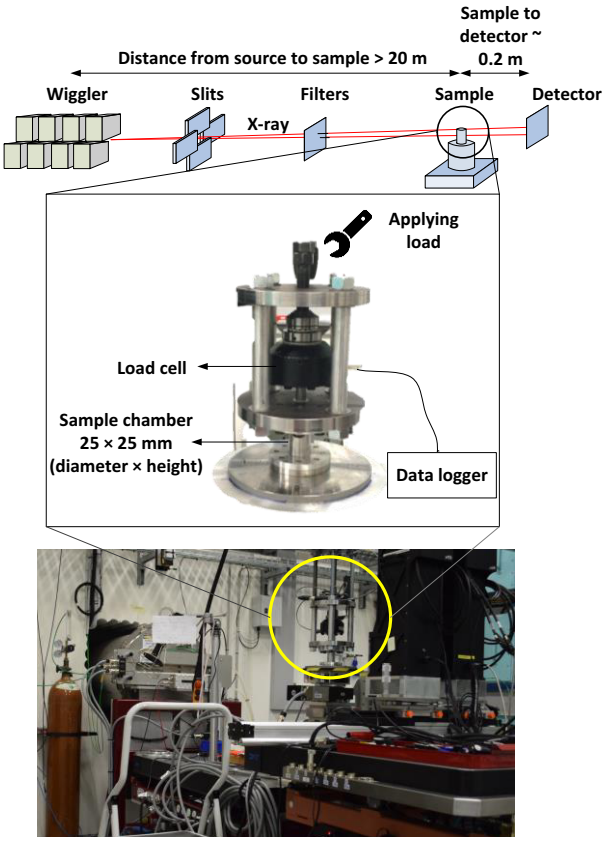

Fig. 1. Schematic diagram of the experimental layout and the loading setup used for the experiments.

3 Grain property evolution due to breakage

In order to gain a better understanding of soil behaviours in relation to grain-scale damage, the changes to the grading and grain morphology of a sand specimen were examined. A uniformly graded sand specimen, 1.18 mm < grain diameter d < 2.36 mm, was scanned under 0, 2.5, 5, and 10 kN compressive loading (i.e. 0, 5.1, 10.19, and 20.38 MPa). The grain size and shape distribution after each loading sequence were obtained from precise 3D reconstruction of 2159 CT horizontal slices using Avizo 9 (Figure 2a-insert). Image processing techniques including image thresholding, filtering, and segmentation, were used to separate and label each fragment in the assembly.

3.1 Soil grading and fractal distribution

While initial grain size distribution is one of the main factors governing the mechanical behaviour of a granular assembly, the way it changes under loading can predict the material behaviour, especially the potential for further breakage. The grain size distribution of the confined sand assembly under different compressive loading is illustrated in Figure 2a. Only fragments with a diameter larger than 0.075 mm were analysed due to inaccuracy in segmenting and evaluating characteristics of extremely small fragments. After scanning under 10 kN loading, the sample was recovered and put through sieve analyses. As shown in Figure 2a, there is a slight discrepancy between grain size distribution measured by 3D reconstruction of the sample and the results from the sieve analysis, particularly between the fine contents. This discrepancy is related to the loss of fine grains during extruding the sample from the chamber at the end of the scanning.

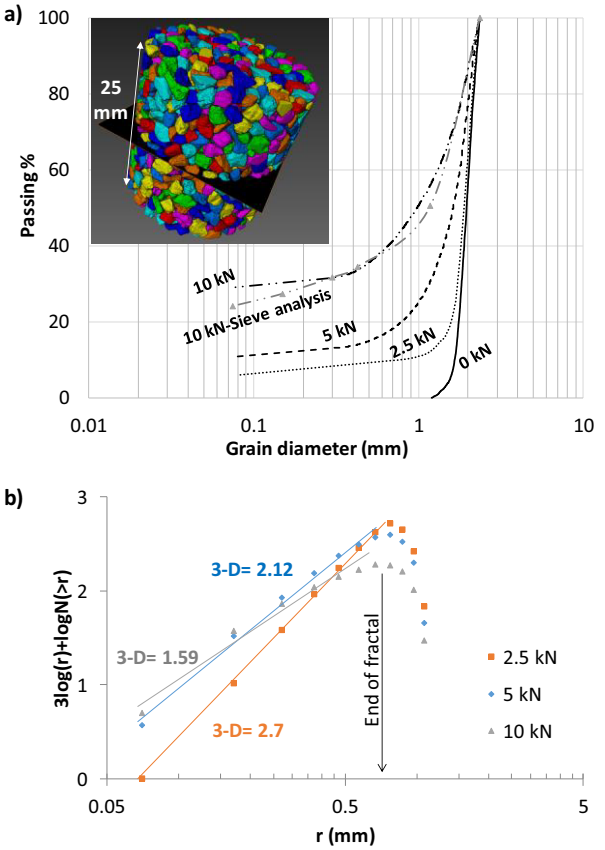

Fig. 2. Sand specimen under different loading levels (0, 2.5 kN, 5 kN, and 10 kN): a) Changes in grain size distribution, b) The fractal distribution.

The sample grading clearly changed from uniform to a well graded distribution as stress increased and breakage progressed further (Figure 2a). Altuhafi and Coop [4] also reported that toward the terminal state, the soil gradation eventually tends to shift to well-graded, which explains the fact that very well-graded and fractal soil experiences no dramatic breakage. Fractal theory, first used by Hartmann [8] to study crushing processes in meteorites, is widely used to quantify the amount of breakage occurring under loading or after large displacement. It is widely accepted that fragmentation is a fractal phenomenon suggesting that it is also a scale-invariant mechanism, and the fractal dimension (D) describes the changes in grain size distribution. Referring to Eq. 1, the original fractal dimension can be calculated based on number of grains, i.e. $N(>r)$ which is the cumulative number of fragments with radius larger than r [9]. However, due to the difficulty in counting grains, Einav [2] proposed a method based on the mass of grains smaller than a certain size.

$$3\log(r) + \log N(>r) \propto (3-D)\log(r) \qquad (1)$$

With the aid of CT scanning, numbers of grains and newly generated fragments were directly and precisely measured. The radius was calculated by measuring the volume of each grain and defined as the radius of a sphere having the same volume as the grain. The fractal condition is clear in Figure 2b which shows (*3-D*) from Eq. 1, and the fractal dimension rises from 0.3 to 1.41 with the increase in compressive stress, confirming that as further breakage happens in the sample the gradation tends to be more fractal. This is the same trend observed by Turcotte [10], Einav [2], and Zhao et al. [9]. Nevertheless, it seems some large grains did not experience remarkable fragmentation, and the fractal region has ended for grains with diameter above 1.5 mm; at all stress levels the upper bound of fractality is the same. This observation contrasts with the notion of size effects in strength of material, where breakage survival probability of a grain decreases as its size increases [11]. McDowell, Bolton and Robertson [12] also stated that while crushing strength of a grain depends on its size, high coordination number (number of neighbouring grains) reduces the probability of grain fractures, and attempts to model grain breakage based on these two effects (i.e. grain size and coordination number) are very limited. Therefore, the termination of fractality in Figure 2b is related to the fact that when stress increases, more fine fragments are generated by breakage, resulting in a denser packing and higher coordination number around the larger grains. Consequently, breakage becomes more dominant in smaller grains and less likely for larger ones.

3.2 Morphology

Statistical and quantitative analyses of 3D labelled images are presented in Figures 3 and 4 in terms of grain shape/morphology evolution. Figure 3a shows the changes in Aspect Ratio (AR) distribution due to breakage, which is the ratio of the short axis of the best fitted ellipsoid to its long axis. Figure 3b demonstrates the true sphericity distribution, defined as the ratio of the surface area of a sphere having the same volume as the fragment to the actual surface area of the fragment [13]. Figure 3 indicates that after the first loading sequence (2.5 kN or 5.1 MPa) both AR and true sphericity increased. This observation suggests that grains show a tendency to move away from morphological extremes during crushing. Abbireddy and Clayton [14] also reported similar results on changes in grain forms during a triaxial shear test. Nonetheless, under higher levels of stress a reverse trend was observed in both true sphericity and aspect ratio distributions as both of these shape factors tend to decrease (Figure 3). Figure 4 also illustrates the evolution of mean values of AR and true sphericity versus Hardin's relative breakage, which is calculated as the ratio of total breakage to breakage potential (more information can be found in Hardin [15]). A slight decrease in the mean value of true sphericity and a more notable drop in average AR were measured at higher stress levels (i.e. 5 kN or 10.19 MPa and 10 kN or 20.38 MPa). It is interesting that newly created fragments under higher stress levels are less spherical and have lower aspect ratios than the initial grains. Takei et al. [16] and Zhao et al. [9] also noted slight reduction in sphericity and AR of different individual grains in a single particle crushing test. Referring to Figure 3a, despite the severe fragmentation under 10 kN loading, no noticeable change was measured in the fragments' AR compared to the AR distribution of fragments generated under 5 kN loading, supporting the notion of a terminal state [17]. Furthermore, to quantify the uniformity of shape distribution, the Relative Distribution Factor (*RDF*) was calculated for each shape factor distribution (Eq. 2):

$$RDF=AR_{90}/AR_{10}$$

$$RDF=True\ Sphericity_{90}/\ True\ Sphericity_{10} \quad (2)$$

where AR_{90} and AR_{10} or $True\ Sphericity_{90}$ and $True\ Sphericity_{10}$ are the value of shape factor at which 90% and 10% of fragments have a smaller value, respectively. Figure 4 reveals that at first there has been a slight fall in *RDF* of AR, and a larger fall in *RDF* of true sphericity. This means that the grains during the first phases of splitting and breakage tend to create fragments with approximately uniform shapes. Afterwards, *RDF* of both shape factors tend to gradually increase while the sample was experiencing more severe fragmentation under higher loading level. This implies that due to the complex mechanisms of breakage, during severe fragmentation newly generated fragments have more diverse shapes. It should also be noted that true sphericity at every loading stage distributed normally with equal mean, median, and mode values. On the contrary, considering the skewness of AR distribution shown in Figure 3a, the distribution tends to skew to the right, toward lower values of AR, with increased crushing in the sample.

Overall, morphological changes during breakage showed a reversal trend as stress increased, with a shift from more spherical and bulky to less spherical and flaky shapes.

3.3 Particle shape versus size

The literature shows that particle size and shape are interrelated. Domokos et al. [18] showed that the shape of fragments generated under (significant) dynamic loading on 'large' 15-150 mm particles obeys universal scaling laws and that the larger crushed particles tend to be elongated. However, Altuhafi and Coop [4] and Sun et al. [19] obtained contrasting results (increase in sphericity and aspect ratios of sand and ballast particles as particle size increased), for smaller diameter particle assemblies under different crushing loads than that of [18].

Figure 5 shows AR of newly generated fragments in relation to their size, i.e. fragment diameter. Particles with d>1.5 mm were removed from the analysis since they did not experience fragmentation (Section 3.1). The figure shows a slight decrease in AR as fragment size decreases, in line with [4] and [19].

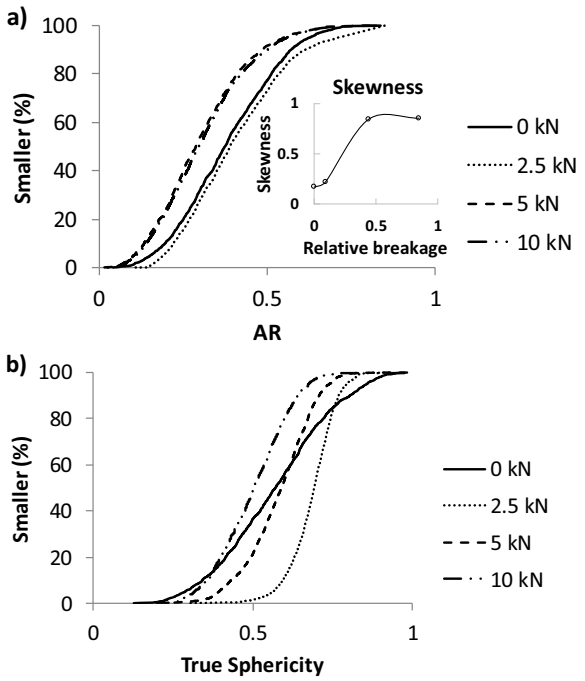

Fig. 3. Morphology evolution of the sand grains under different loading levels: a) Aspect Ratio, b) True sphericity distribution.

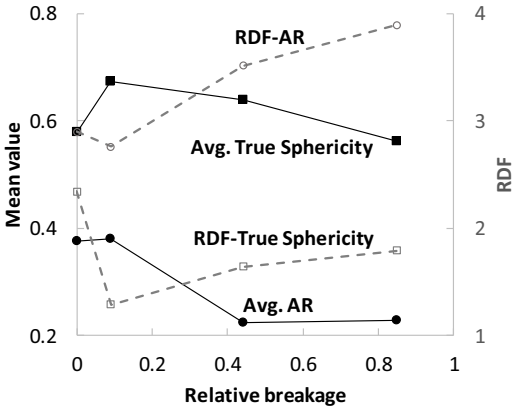

Fig. 4. Changes in statistical properties of shape factor distributions of sand fragments due to breakage: Mean values of AR and true sphericity, and Relative Distribution Factor.

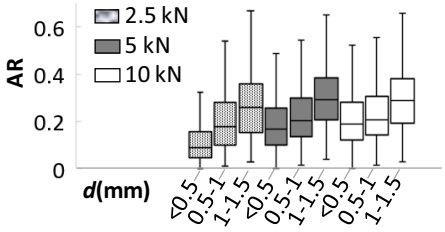

Fig. 5. Relationships between Aspect Ratio and particle size.

Conclusion

A novel loading apparatus was developed to perform constraint compression tests on a sand specimen while being scanned using cutting-edge Synchrotron tomography. Synchrotron tomography was used to study alterations in grain characteristics of a sand specimen. The fractal distribution of the sand assembly due to breakage demonstrated that breakage becomes dominant in smaller grains rather than larger ones where an increase in the amount of newly generated fine fragments causes high coordination number surrounding the larger grains.

The results of morphological changes also reveal that there is a reversal trend in the grain shape evolution with increasing stress. The sand grains tended to generate more spherical fragments with higher aspect ratio whereas by increasing the stress this trend reversed. Due to severe breakage and splitting under higher stress levels, less spherical fragments with lower aspect ratio compared to the original grains were created.

This research was undertaken on the Imaging and Medical Beam Line at the Australian Synchrotron, Victoria, Australia.

References

1 Y. Ghorbani, M. Becker, J. Petersen, S. H. Morar, A. Mainza, and J.-P. Franzidis, Minerals Engineering **24** (12), 1249 (2011).
2 I. Einav, Journal of the Mechanics and Physics of Solids **55** (6), 1274 (2007).
3 W. Zheng and D. D. Tannant, Canadian Geotechnical Journal (ja) (2016).
4 F. Altuhafi and M. R. Coop, Géotechnique **61** (6), 459 (2011).
5 T. Afshar, M. M. Disfani, A. Arulrajah, G. A. Narsilio, and S. Emam, Powder Technology **308**, 1 (2017).
6 M. B. Cil and K. A. Alshibli, Géotechnique **64** (5), 351 (2014).
7 C. Hall, D. Hausermann, A. Maksimenko, A. Astolfo, K. Siu, J. Pearson, and A. Stevenson, Journal of Instrumentation **8** (06), C06011 (2013).
8 W. K. Hartmann, Icarus **10** (2), 201 (1969).
9 B. Zhao, J. Wang, M. Coop, G. Viggiani, and M. Jiang, Géotechnique **65** (8), 625 (2015).
10 D. Turcotte, Journal of Geography Research **91** (12), 1921 (1986).
11 D. R. Jones and M. F. Ashby, *Engineering materials 2: an introduction to microstructures, processing and design*. (Butterworth-Heinemann, 2005).
12 G. McDowell, M. Bolton, and D. Robertson, Journal of the Mechanics and Physics of Solids **44** (12), 2079 (1996).
13 H. Wadell, The Journal of Geology, 250 (1935).
14 C. Abbireddy and C. Clayton, Granular Matter **17** (4), 427 (2015).
15 B. O. Hardin, Journal of Geotechnical Engineering **111** (10), 1177 (1985).
16 M. Takei, O. Kusakabe, and T. Hayashi, Soils and Foundations **41** (1), 97 (2001).
17 A. Narsilio and J. Santamarina, Geotechnique **58** (8), 669 (2008).
18 G. Domokos, F. Kun, A. Á. Sipos, and T. Szabó, Scientific reports **5**, 9147 (2015).
19 Y. Sun, B. Indraratna, and S. Nimbalkar, Géotechnique Letters **4** (July-September), 197 (2014).